

OXFORD JOURNALS

Radiation Protection Dosimetry

The Dose from Compton Backscatter Screening

| | |
|---------------------|--|
| Journal: | <i>Radiation Protection Dosimetry</i> |
| Manuscript ID: | RPD-10-0234 |
| Manuscript Type: | Paper |
| Subject Index Term: | Backscatter, Dose equivalent/effective dose etc., Dosimetry: physical basis, Low dose radiation, Models/modelling, Personnel/individual monitoring, Population exposures, X rays |
| | |

SCHOLARONE™
Manuscripts

Review

The Dose from Compton Backscatter Screening

Peter Rez,^{*} Robert L. Metzger[#] and Kenneth L. Mossman[†]

All correspondence should be sent to:

Professor Peter Rez

Department of Physics

Arizona State University

Tempe, AZ 85287-1504

Phone: 480.965.6449

Fax: 480.965.7954

Email: peter.rez@asu.edu

^{*} Department of Physics, Arizona State University, Tempe, AZ 85287-1504

[#] Radiation Safety Engineering, Inc., 3245 N. Washington St, Chandler, AZ 85225

[†] School of Life Sciences, Arizona State University, Tempe, AZ 85287-4501

Abstract

Systems based on the detection of Compton backscattered X-rays have been deployed for screening personnel for weapons and explosives. Similar principles are used for screening vehicles at border crossing points. Based on well-established scattering cross sections and absorption coefficients in conjunction with reasonable estimates of the image contrast and resolution the entrance skin dose and the dose at a depth of 1 cm can be calculated. Effective dose can be estimated using the same conversion coefficients as used to convert exposure measurements to effective dose. We show that effective dose is highly dependent on image resolution (i.e., pixel size). The effective doses for personnel screening systems are unlikely to be in compliance with the ANSI standard NS 43.17 unless the pixel sizes are greater than 4 mm. Nevertheless, calculated effective doses are well below doses associated with health effects.

Key words: American National Standards Institute (ANSI), Compton backscatter, dose assessment, X-ray screening

INTRODUCTION

Since the September 2001 terrorist attacks, there has been considerable interest in the development and deployment of personnel screening systems that will detect explosives and other contraband as well as metal objects. With over 700 million airline passengers per year in the US, screening technology must be fast and accurate¹. Systems based on millimeter wave scattering and large angle Compton scattering are being used at airports and other facilities, including prisons and detention centers, around the world. In X-ray scanning, a passenger is scanned by moving an X-ray beam rapidly over the body. The signal strength of detected backscattered X-ray allows a highly realistic surface image to be reconstructed. Screening is rapid and image resolution of the technology is high.

The deployment of X-ray screening units in major airports around the country has raised concerns about radiation doses to passengers. Although dose calculations are not publicly available from screening system vendors their claims of compliance with the 2002 American National Standards Institute (ANSI) standard can be interpreted to mean that effective doses to passengers are 0.1 μSv or less. In 2002 ANSI set a standard of 0.1 μSv per scan for an individual². In 2009 ANSI relaxed the 2002 standard from 0.1 to 0.25 μSv per “screening” as applied to “general use” systems. The reason for changing from a per-scan limit to a per-screening limit is to be fair to transmission systems that require only one scan versus multiple scans³. An effective dose of 0.25 μSv is substantially less than the average effective dose of 6.2 mSv members of the US population get every year from all sources of radiation exposure, and is less than the increased cosmic radiation dose passengers receive during commercial airline travel⁴

There are two systems in widespread operation, the significant difference between them being the peak X-ray energy (kVp). The lower energy system has an X-ray source operating at 50kVp giving X-rays of average energy 28keV, while the X-ray source for the higher energy system operates at 125kVp, and the average X ray-energy is about 60keV. There is also a vehicle scanning system that uses an even higher energy 450 kVp X-ray generator. Although vendor-determined doses are small and not associated with adverse health effects dose accuracy is in question because of inherent difficulties in measuring X-ray exposures from rapidly moving X-ray beams. Hupe and Ankerhold^{5,6} measured doses from cargo screening and personnel screening systems. Their dose estimates for the Compton backscatter personnel screening system were 2 times higher when they used a specially constructed ionization chamber and associated electronics as opposed to a commercially available proportional counter. Furthermore, doses should be kept as low as reasonably achievable because of the large number of airline passengers screened annually. In this paper we use the theory of image formation and well established scattering cross sections and absorption coefficients to estimate effective dose. Our findings indicate effective doses may be as high as 0.8-0.9 μSv for the personnel screening systems. This is about 4 times higher than the maximum value determined by the vendors as indicated by their claims that doses are in compliance with the ANSI 2002 standard of 0.1 μSv per scan (assuming 2 scans per passenger). The increased dose to individual passengers remains well below doses that are known to cause adverse health effects.

DOSE ESTIMATION

The outlines of a Compton backscatter screening system for personnel were given in the patent application of Smith⁷. The essential features of the system are shown as Fig.

1. An X-ray tube with a collimator is used to generate a fan beam of X-rays, and a chopper wheel further restricts the X-rays to a pencil beam that scans in the vertical plane. The dose can be estimated from the image quality. The quality of the image sets requirements (lower limits) on the number of X-rays detected for each pixel and the Compton scattering cross section can be used to estimate the number of incident X-rays per pixel.

The dose can then be calculated from published data relating dose to fluence⁸ or Monte Carlo calculations. As Smith⁷ stated in his patent application the pixel size is critical. From features shown in published images in a report on the higher energy system^{4,9} (it would appear that the pixel size is 2mm (features on the gun and the zipper set these limits). The 2mm pixel size also is consistent with 1000 pixels in 2m, or 500 in 1m which would be appropriate for computer display of an individual. In one image it would appear that the pixel size is 1mm from features on a gun and the wire frame of glasses.⁹ In the image shown from the lower energy system resolution of the chain and the frame of the glasses would also indicate a 2mm pixel size.⁴ From magnified images of the vehicles a reasonable estimate of the pixel size for the vehicle scanning system would be 2cm.

As a first step in our calculation the x-ray fluence required to give a peak image intensity (showing as white on a displayed image) will be estimated. The general expression for the Compton backscattered signal picked up at a point \mathbf{r}' in the detector from a beam passing through points along the vector connecting \mathbf{r}_1 to \mathbf{r} is

$$I = \iint \exp(-\mu_f |\mathbf{r}_2(\mathbf{r} - \mathbf{r}') - \mathbf{r}|) \frac{d\sigma}{d\Omega} I_0 N_e \exp(-\mu_i |\mathbf{r} - \mathbf{r}_1(\mathbf{r} - \mathbf{r}_0)|) \frac{d^2 r'}{|\mathbf{r} - \mathbf{r}'|^2} d\mathbf{r} \quad (1)$$

where \mathbf{r}_2 is the point on the surface of the person on the line connecting \mathbf{r}' to \mathbf{r} and \mathbf{r}_1 is the point on the surface of the person connecting \mathbf{r}_0 on the X-ray source to \mathbf{r} , as shown in Figure 1. In equation 1 I_0 is the incident number of X-rays, N_e is the number of electrons per unit volume, μ_i is the absorption coefficient for the incident X-rays, μ_f the absorption coefficient for the Compton scattered X rays and $\frac{d\sigma}{d\Omega}$ the Compton differential scattering cross section. To evaluate with a very high degree of precision would require a model for a human phantom, and detailed engineering diagrams showing the arrangement of the X-ray source and detectors.

Instead the maximum volume that could contribute to the signal will be estimated.

Neglecting the curvature of the person being scanned, equation 1 becomes

$$I = \iint \exp\left(-\mu_f \frac{z}{\cos \theta_f}\right) \frac{d\sigma}{d\Omega} N_e I_0 \exp\left(-\mu_i \frac{z}{\cos \theta_i}\right) \frac{d^2 r'}{|\mathbf{r} - \mathbf{r}'|^2} d\mathbf{r} \quad (2)$$

where z is a distance beneath the surface. To further simplify this expression the integration over the paths to the detector will be replaced by an effective solid angle, $\Delta\Omega$.

Equation 2 now becomes

$$I = \int_0^{\infty} N_e \frac{d\sigma}{d\Omega} \Delta\Omega I_0 \exp\left(-\left(\frac{\mu_i}{\cos\theta_i} + \frac{\mu_f}{\cos\theta_f}\right)z\right) dz \quad (3)$$

The absorption coefficients are about 0.15-0.2 cm²/gm giving an effective absorption depth of 5-6 cm which means that the integration through the body can be taken to infinity. As a last approximation the cosine factors will be set equal to 1 and the resulting integration gives

$$I = \frac{N_e \Delta\Omega I_0}{(\mu_i + \mu_f)} \frac{d\sigma}{d\Omega} \quad (4)$$

Note that this approximation leads to a higher estimation for the detected signal and therefore a lower estimate for the incident fluence. This means that the dose estimates given below might be a factor of 2 -3 too low.

Rearranging equation 4 to get I_0 , we have

$$I_0 = \frac{I(\mu_i + \mu_f)}{N_e \Delta\Omega \frac{d\sigma}{d\Omega}} \quad (5)$$

The Compton scattering cross sections can be calculated from the Klein Nishina formula^{10,11} and as shown in Fig. 2 the differential cross section becomes more forward peaked as the energy increases. The cross section for backscattering decreases as the energy is increased. From the footprints of both the personnel screening systems it would appear that the scattering angle is 135°. This angle is not critical since the cross section varies slowly in this region. The higher energy system uses 125 kV x-ray generator with a tungsten target. From a calculated X-ray spectrum the average X-ray energy is 60 kV and the differential cross section for Compton scattering is $4.23 \times 10^{-26} \text{ cm}^2$. In the case of the lower energy system the average X-ray energy is 28 kV and the Compton scattering differential cross section is $5.01 \times 10^{-26} \text{ cm}^2$. The vehicle scanning system uses a higher energy X-ray generator with 450 kV. The average X-ray energy can be estimated from the image of the driver sitting in a truck with the window down. The image intensity of the arm is attenuated by a factor of 33% by transmission through the door and window. Using X-ray absorption coefficients from XCOM¹⁴ and assuming the door is 1mm steel and the glass is 6mm thick the average energy for the incident X-rays is 200 keV. The differential cross section for Compton scattering relevant for the vehicle scanning system is $2.52 \times 10^{-26} \text{ cm}^2$.

The footprint of both the low energy and high energy systems suggest that the scintillators are on either side of the person being scanned and have a total area of about 1m^2 . The solid angle varies between 0.6 sr for a point near the feet or the head to 1.0 sr for a point in the center of the body. In the design of the low energy system the effective scintillator area is increased because the scintillator panels are inclined at an angle of approximately 20° to the front face, and the total scintillator area is closer to 1.6m^2 . The solid angle now varies between 1.0 sr for a point near the head or feet to 2.0 sr for a point near the center of the body.

The number of counts can be estimated from the fluctuations in a constant area in the published images. In a region of high intensity near the center of the body the fluctuation in intensity is about 5 units on 200 units. This would imply 40 intensity levels, requiring 1600 X rays incident on the detector for a perfect detection system, detection quantum efficiency (DQE) 1. In reality the DQE would be closer to 0.5 (even this is optimistic) and about 3200 X rays would be required. For intensity fluctuations of 10 in 200 units the peak number of X rays per pixel incident on the detector would be 800 if the DQE were 0.5. If an 8 bit A/D converter were used and the system with a perfect detector really did discriminate 256 levels then 64,000 counts would be required (\sqrt{N} uncertainty, 1σ), though its very unlikely the systems operate with this high degree of level discrimination.

The energy of the Compton scattered X-ray, E_f , is lower than the incident energy, E_i and is given by

$$E_f = E_i - m_0c^2(1 - \cos\theta) \quad (6)$$

The absorption coefficient is therefore higher. Absorption coefficients from XCOM¹⁴ for 28 kV, 60 kV and 200 kV incident X-rays are given in Table 1 below.

The numbers of incident X-rays can be calculated from equation 5 and are shown in Table 2. for a point near the center of the body where the collection solid angle is greatest and hence the number of incident X-rays is least.

In all cases Compton scattered X-rays are approximately 4 % of the number of incident X-rays. Monte Carlo simulations using the Penelope code¹³ confirm these estimates from the simple theory.

Although high, the numbers for incident photons per pixel are reasonable. The higher energy personnel screening system completes a scan in about 8 sec. That means the dwell time per pixel is about 15 μ sec per pixel which corresponds to 3.3×10^8 photons per second. The scanning beam solid angle is 8×10^{-6} for 2mm pixels if the person is about 0.7 m from the X-ray source⁵. Monte Carlo calculation using Penelope indicate that 125kV electrons incident on a tungsten target give 2.5×10^{-3} X-rays per sr. The tube current required to produce the needed fluence is 3.5 mA, consistent with the data in NCRP Commentary No. 16.⁴

To calculate the dose the fluence has to be calculated from the number of incident photons per pixel and the pixel size. The dose, D , in μGy is given by

$$D = \frac{I_0}{\Delta x^2} F \quad (7)$$

where Δx is the pixel size in mm and F is the dose in μGy per unit fluence in X-rays incident per mm^2 . The NS 43.17 standard uses data for F from tables published by Birch et al.⁸ The conversion factor, F , can also be derived from Monte Carlo calculations. The Penelope code was used for both a parallel beam of X-rays incident on a 25 cm water slab and for a point X-ray source 100 cm away with X-rays confined to a 5° semi-angle cone. There was very little difference using either of these two methods and the results, along with the values from Birch et al.⁸ are summarized in Table 3.

It is not surprising that the dose per unit incident fluence is lowest for the higher energy screening system with an average energy of 60kV. This is the window used for radiology; it also has significant contrast from photo-absorption. At higher energies the lower absorption is compensated by the higher energy absorbed; at lower energies the higher absorption means that the energy is deposited in a smaller mass.

Using equation 7 the entrance skin absorbed dose and the dose at 1cm depth (in μGy) can be calculated for the personnel screening and the vehicle portal system.

Entrance doses are not necessarily the highest doses. Peak doses would occur at depth corresponding to the build-up distance. The entrance skin dose is much higher for the

lower kVp personnel screening systems, due to the increased absorption of lower energy X-rays.

For comparisons with vendor estimated effective doses and the ANSI standard, absorbed doses were converted to effective doses as shown in Table 4 using effective dose conversion factors provided as Figs C1 and C2 in ANSI 43.17.³ These conversion factors are based on a Monte Carlo model that converts a measured exposure or air kerma to an effective dose. The effective doses in Table 4 reflect multiple projections. Since anterior and posterior views are taken for the personal screening systems the calculated dose per screening is the sum of the effective doses for each view. Since there are no dose conversion factors provided for the high energy vehicle scan system a conservative estimate was made based on unit conversion factors. The entrance skin dose was multiplied by three since 3 views are taken for a complete screening

The use of effective dose favors the lower energy systems even though the entrance skin dose can be very much higher. This has been recognized in the standard.³

“However, it was desired to preserve a system of dose limitation that would not penalize systems using lower energy x-rays. These systems generally deliver a lower effective dose per scan while the measured air kerma or entrance skin dose may be higher than systems operating at higher energy.”

As can be seen from equation 7 and Figs 3a and 3b the absorbed dose is linearly proportional to the peak number of scattered photons needed for adequate contrast and inversely proportional to the pixel area. Due to the large pixel size in the vehicle scanning system, a consequence of the large source-target distance, the vehicle scanning system gives doses below the revised ANSI standard of 0.25 μSv at 3200 peak X-rays incident on the detectors per pixel. For high resolution detail the lower energy personnel

screening systems, even under optimistic assumptions for detection efficiency, exceed the revised ANSI standard at 3200 peak X-rays incident on the detectors per pixel. This is due mainly to the high concentration of radiation in a small area. If the resolution were degraded to about 4mm per pixel the effective dose for the personnel screening system would be below 0.25 μSv per screening. Uncertainties in these estimates mainly come from the range of detector solid angles, a reduction by a factor of 2 corresponding to a point at the feet or the head of the individual would double the dose. As can be seen from Table 3 use of the Birch et al.⁸ conversion factors for calculating dose from fluence would reduce the dose by a factor of almost 2 for the personnel screening systems. The next largest source of uncertainty is the average scattering angle, but as can be seen from Fig 2, this can at most cause a variation of $\pm 10\%$, though it could be as high as $\pm 25\%$ for the lower energy system. In comparison the Klein Nishina scattering cross section and the absorption coefficients have negligible uncertainty. It should also be remembered that these same absorption coefficients are used to convert ionization chamber measurements to dose and will therefore be present in experimental measurements.

NCRP Commentary No. 16 provides radiation protection advice (including radiation levels during screening) concerning ionizing radiation-producing devices that are being evaluated by federal agencies for uses in screening of humans for the purpose of security⁴. The effective doses per scan reported by NCRP (0.05 μSv per scan for anterior plus posterior views) are lower than our calculated doses. NCRP reported measurements of exposure from X-ray beams as described in the ANSI standard published document.² The dosimetry techniques advised using a large ion chamber (at least 1500cc) as the

expected doses were very low. Calibration of a large volume ionization chamber for this partial volume irradiation condition is also difficult. With the chamber positioned at the passenger skin entrance, less than one percent of the chamber volume is irradiated per sweep of the beam. Ion chambers are typically calibrated with the chamber fully covered by the incident x-ray beam. The behavior of the chamber under partial volume irradiation by a rapidly moving x-ray spot is difficult to estimate, and no commercial calibration facility offers a calibration geometry that mimics this challenging exposure condition. Large ion chambers are also limited in dose rate. For example the Radcal Accupro 10x6 1800cc ion chamber has is specified for a maximum dose rate of 0.2 mGy/sec¹⁵. This will be exceeded for an air kerma greater than 0.003 μ Gy for a pixel time of 15 μ sec. This value is much less than the air kerma that would be measured even if the system met the standard.

CONCLUSIONS

While the vehicle portal system is probably in compliance with the 0.25 μ Sv ANSI standard, it is highly unlikely that the dose from the personnel screening systems are in compliance if the pixel size were 2mm and the number of photons incident on the detectors is 3200 per pixel. They could well be in compliance if the resolution were only 4 mm or if only 800 photons were incident on the detectors. Nevertheless increased doses to large populations beg the question of potential public health effects.

The major public health effect of concern at low doses of ionizing radiation is cancer. There is clear evidence of cancer induction at effective dose above about 200 mSv. Below an effective dose of about 100 mSv radiogenic cancer mortality risk estimates for all cancers is highly uncertain.¹⁶ It is not possible to determine reliably whether a radiogenic risk is present in an X-ray screening population because of the high spontaneous incidence of cancer and multifactorial nature of disease causation¹⁷.

Use of collective dose to estimate public health impacts when large populations are exposed to trivial doses is inappropriate and not reasonable. The assumptions implicit in the collective dose calculation conceal large biological and statistical uncertainties.¹⁶ If an individual passenger is not harmed by X-ray screening then the population isn't either.

Passenger screening presents no public health concern under normal operating conditions. However, serious consideration should be given to the possibility of unintended and unnecessary doses to passengers due to malfunctioning equipment. The NS 43.17 standard requires the exposure terminate before an effective dose of 0.25 mSv is reached if the scanning mechanism were to fail. This means the fail-safe mechanism must detect the fault and shut off the beam within a period of about 15 msec. If this system also malfunctions (and failure of fail-safe mechanisms are not unknown), there may be a significant delay (of the order of tens of seconds) before the operators noticed something was wrong, especially given the fact that the screener viewing the image is in a remote location. Under these conditions the passenger could receive a high localized

dose of a few sievert. High doses are associated with deterministic effects including skin erythema .

ACKNOWLEDGEMENTS

The authors thank Dr. Steven Smith for very helpful correspondence, Dr Leon Kaufman for sharing unpublished results with us and Jon Mull for help with the figures.

For Peer Review

REFERENCES

1. Bureau of Transportation Statistics, *National Transportation Statistics* , U.S. Department of Transportation Research and Innovative Technology Administration, Bureau of Transportation Statistics (2009). Accessed at:
http://www.bts.gov/publications/national_transportation_statistics/
2. American National Standards Institute (ANSI). Radiation Safety for Personnel Security Systems Using X-rays. American National Standards Institute. N 43.17, (2002).
3. American National Standards Institute (ANSI). Radiation Safety for Personnel Security Screening Systems Using X-ray or Gamma Radiation. American National Standards Institute N43.17 Approved: August 2009.
4. National Council on Radiation Protection and Measurements. Screening of Humans for Security Purposes Using Ionizing Radiation Scanning Systems. NCRP Commentary No. 16, Bethesda, MD: NCRP; (2003)
5. Hupe, O and Ankerhold, U. Determination of Ambient and Personal Dose Equivalent for Personnel and Cargo Security Screening Rad. Prot. Dosim 121, 429-437 (2006)
6. Hupe, O. and Ankerhold, U. X-ray security scanners for personnel and vehicle control: Dose quantities and dose values Eur. J. Radiol. 6 , 237-241 (2007)

7. Smith, S. W.. X-ray backscatter imaging system including moving body tracking assembly. U. P. Office. USA, Rapiscan Secure 1000 Security Products (1998)
8. Birch, R., Marshall, M. and Adrian, G.M. Catalogue of Spectral Data for Diagnostic X-rays, Scientific Report Series 30. Hospital Physicists Association (1979)
9. Baukus, W. J. X-ray Imaging for On-The Body Contraband Detection. 16th Annual Security Technology and Exhibition. Williamsburg,VA, National Defense Industrial Association, (2000).
10. Heitler, W.. The Quantum Theory of Radiation. (Oxford: Clarendon Press), (1954). reprinted by (Dover,New York), (1984) ISBN 0-486-64458-4
11. Johns, H. E. and J. R. Cunningham The Physics of Radiology. (Springfield,IL: Charles Thomas) (1983) ISBN 0398046697.
12. S Smith, Personal communication, August (2010)
13. Baro, J., Sempau, J., Fernandez-Varea, J.M., Salvat, F. PENELOPE: An algorithm for Monte Carlo simulation of the penetration and energy loss of electrons and positrons in matter, Nucl. Inst. Methods B 100, 31-46 (1995)

14. Berger, M. J., J. H. Hubbell, Seltzer, S.M., Chang, J., Coursey, J.S., Sukumar, R., Zucker, D.S. XCOM: Photon Cross Section Database. Gaithersburg, MD, National Institute for Standards and Technology, (2005).
15. Accupro Specification, <http://www.radcal.com> , consulted July 2010
16. International Commission on Radiological Protection (ICRP). The 2007 recommendations of the International Commission on Radiological Protection. Publication 103. Annals of the ICRP; 2007.
17. American Cancer Society, Cancer Facts & Figures, 2010. Atlanta, GA: American Cancer Society, Inc., 2010

Figure Captions

Fig.1. Schematic diagram of a personnel screening system. The diagram shows a beam at an angle of incidence θ_i entering a person being scanned at position \mathbf{r}_1 , before being Compton scattered at position \mathbf{r} . The scattered beam, at an angle θ_f , leaves the person at position \mathbf{r}_2 and strikes the detector at \mathbf{r}'

Fig. 2. Variation of the differential scattering cross section for Compton scattered X-rays as a function of scattering angle. (in units of $\frac{r_0^2}{2} = 3.97 \times 10^{-26} \text{ cm}^2$ where r_0 is the classical electron radius)

Fig 3a. Variation of effective dose with linear pixel dimension for personnel screening systems

Fig 3b. Variation of effective does with linear pixel dimension for the vehicle scanning system.

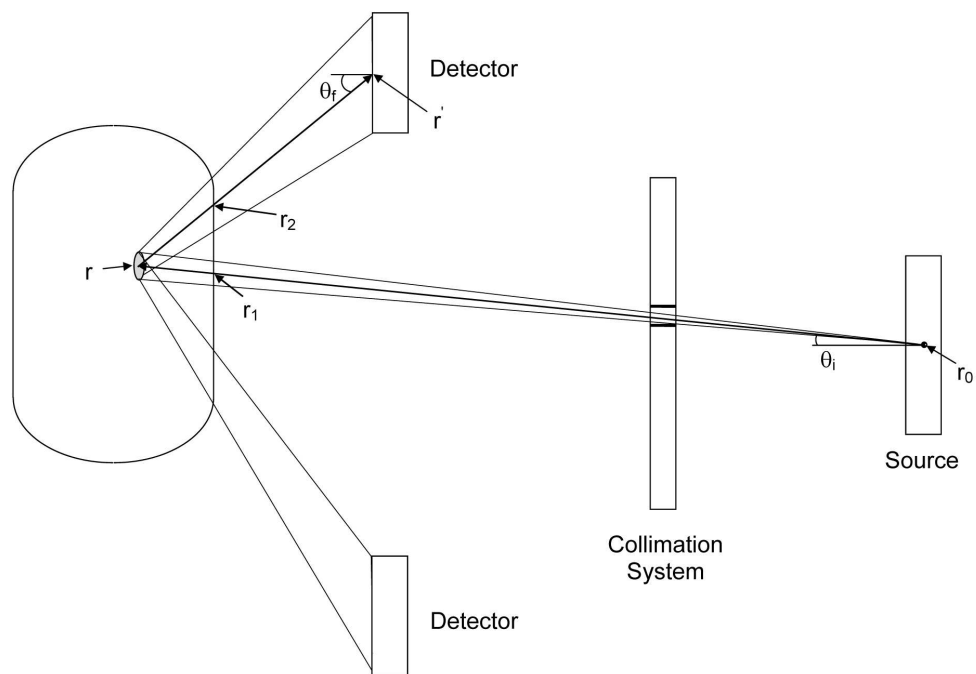
Table Captions

Table 1. X-ray absorption coefficients relevant for Compton backscattering screening systems (given to 3 significant figures, some values interpolated)

Table 2. Incident X-rays per pixel

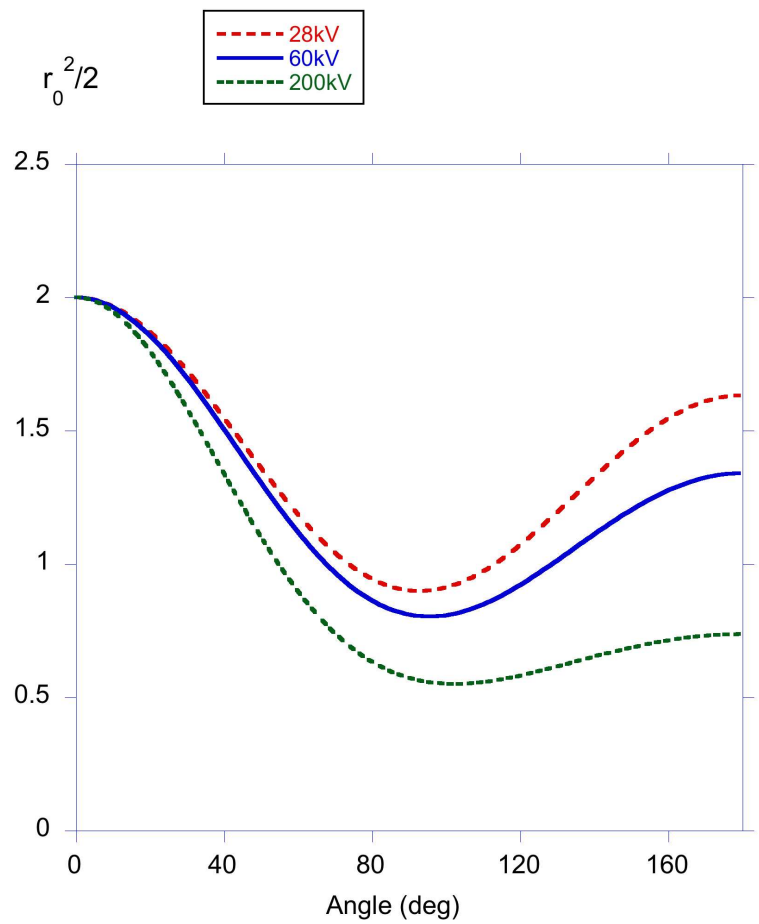
Table 3 Dose in μGy per incident fluence in X rays/ mm^2

Table 4. Entrance skin dose, dose at 1cm depth, conversion factors and effective doses for personnel screening and vehicle portal systems for 3200 peak scattered X-rays incident on the detectors. The conversion factors were obtained from Figs C1 and C2 of NS 43.17 and multiplied by 1.14 55 to convert to $\mu\text{Sv}/\mu\text{Gy}$

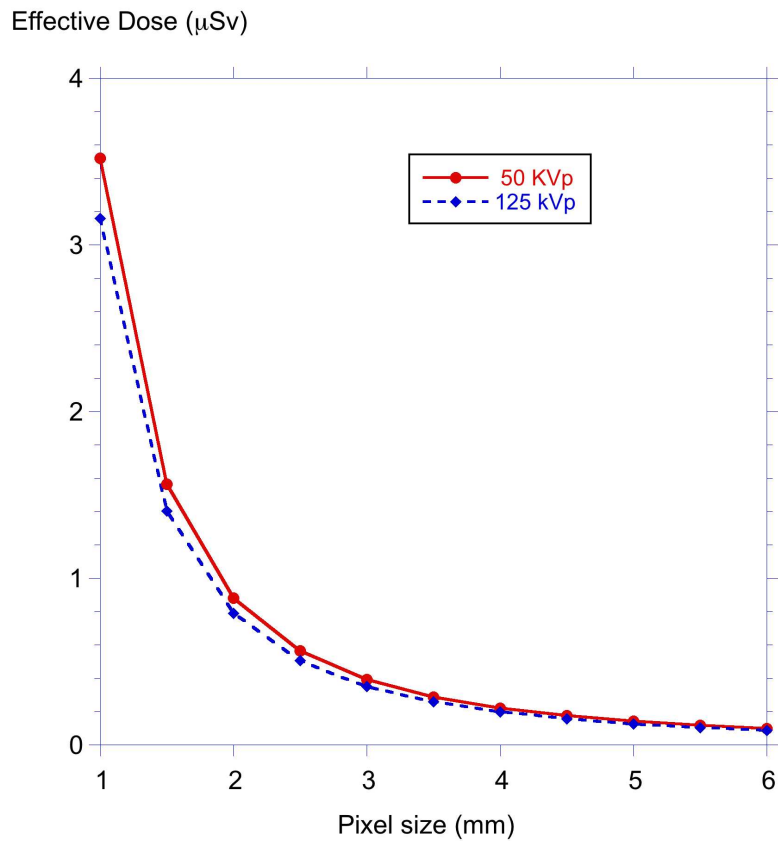


163x109mm (300 x 300 DPI)

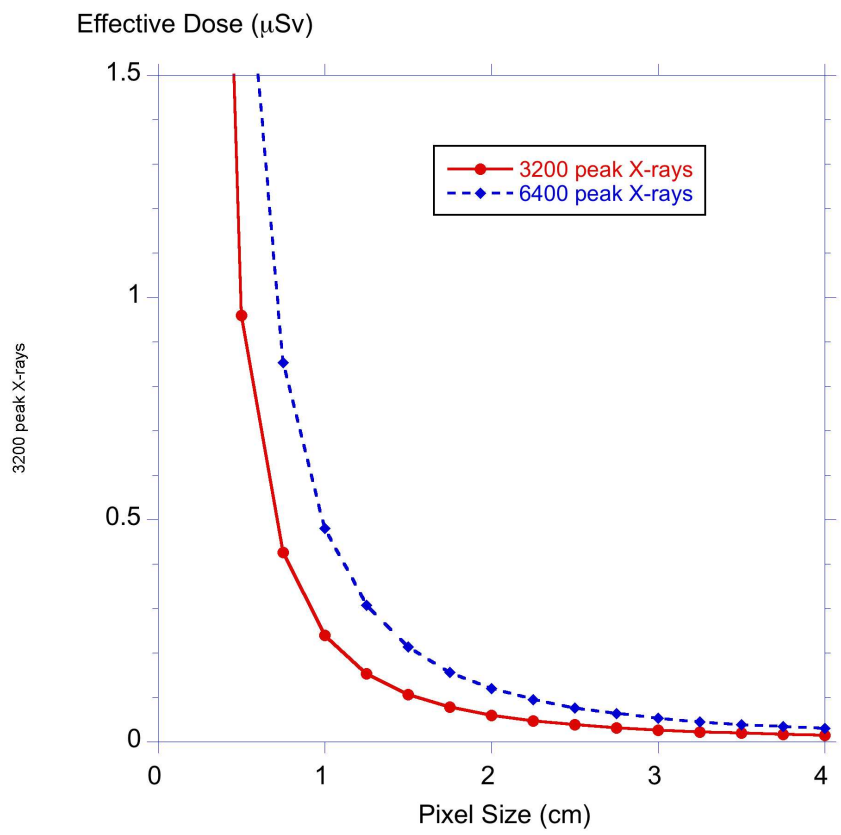
Review



190x190mm (288 x 288 DPI)



190x190mm (288 x 288 DPI)



190x190mm (288 x 288 DPI)

| | Incident X-ray | $\mu_i \text{ cm}^2\text{gm}^{-1}$ | Scattered X-ray | $\mu_f \text{ cm}^2\text{gm}^{-1}$ |
|-------------------|----------------|------------------------------------|-----------------|------------------------------------|
| Low kV Screening | 28 kV | 0.428 | 26 kV | 0.531 |
| High kV Screening | 60 kV | 0.206 | 50 kV | 0.227 |
| Vehicle Portal | 200 kV | 0.136 | 120 kV | 0.163 |

For Peer Review

| Peak X-rays incident on detectors per pixel | Personnel Screening (50 kVp) | Personnel Screening (125 kVp) | Vehicle Portal (450 kVp) |
|---|------------------------------|-------------------------------|--------------------------|
| 3200 | 9.21×10^4 | 4.94×10^4 | 5.68×10^4 |

For Peer Review

| | Personnel Screening (50kVp) | Personnel Screening (125kVp) | Vehicle Scanning (450 kVp) |
|--------------------|-----------------------------|------------------------------|----------------------------|
| Penelope Skin | 1.09×10^{-4} | 6.84×10^{-5} | 1.88×10^{-4} |
| Penelope 1cm depth | 9.13×10^{-5} | 7.37×10^{-5} | 1.97×10^{-4} |
| Birch et al | 6.18×10^{-5} | 3.38×10^{-5} | Not available |

For Peer Review

| | Personnel Screening (50 kVp) | Personnel Screening (125 kVp) | Vehicle Portal (450 kVp) |
|-----------------------------|---------------------------------|----------------------------------|-----------------------------|
| Entrance Skin Dose per scan | 2.5 μGy | 0.68 μGy | 0.019 μGy |
| Dose at 1cm depth per scan | 2.1 μGy | 0.74 μGy | 0.020 μGy |
| Conversion factor A/P | 0.26 | 0.73 | 1.0 |
| Conversion factor P/A | 0.09 | 0.42 | 1.0 |
| Effective Dose | 0.88 μSv | 0.79 μSv | 0.06 μSv |

For Peer Review